The Arabidopsis receptor kinase STRUBBELIG regulates the response to cellulose deficiency

Ajeet Chaudhary[1], Xia Chen[1,3], Jin Gao[1,3], Barbara Leśniewska[1], Richard Hammerl[2], Corinna Dawid[2], and Kay Schneitz[1*]

[1]Plant Developmental Biology, Life Science Center Weihenstephan, Technical University of Munich, Freising, Germany

[2]Chair of Food Chemistry and Molecular Sensory Science, Life Science Center Weihenstephan, Technical University of Munich, Freising, Germany

[3]These authors contributed equally

[*]Corresponding author
Entwicklungsbiologie der Pflanzen
Wissenschaftszentrum Weihenstephan
Technische Universität München
Emil-Ramann-Str. 4
D-85354 Freising
Email: kay.schneitz@tum.de
Tel: +49 8161 715438

Short title: SUB mediates cell wall stress signaling

Key words: cell wall, cell wall damage, cell wall integrity, isoxaben, cellulose

Abstract

Plant cells are encased in a semi-rigid cell wall of complex build. As a consequence, cell wall remodeling is essential for the control of growth and development as well as the regulation of abiotic and biotic stress responses. Plant cells actively sense physico-chemical changes in the cell wall and initiate corresponding cellular responses. However, the underlying cell wall monitoring mechanisms remain poorly understood. In Arabidopsis the atypical receptor kinase STRUBBELIG (SUB) mediates tissue morphogenesis. Here, we show that *SUB*-mediated signal transduction also regulates the cellular response to a reduction in the biosynthesis of cellulose, a central carbohydrate component of the cell wall. *SUB* signaling affects early increase of intracellular reactive oxygen species, stress gene induction as well as ectopic lignin and callose accumulation upon exogenous application of the cellulose biosynthesis inhibitor isoxaben. Moreover, our data reveal that *SUB* signaling is required for maintaining cell size and shape of root epidermal cells and the recovery of root growth after transient exposure to isoxaben. *SUB* is also required for root growth arrest in mutants with defective cellulose biosynthesis. Genetic data further indicate that *SUB* controls the isoxaben-induced cell wall stress response independently from other known receptor kinase genes mediating this response, such as *THESEUS1* or *MIK2*. We propose that *SUB* functions in a least two distinct biological processes: the control of tissue morphogenesis and the response to cell wall damage. Taken together, our results reveal a novel signal transduction pathway that contributes to the molecular framework underlying cell wall integrity signaling.

Author Summary

Plant cells are encapsulated by a semi-rigid and biochemically complex cell wall. This particular feature has consequences for multiple biologically important processes, such as cell and organ growth or various stress responses. For a plant cell to grow the cell wall has to be modified to allow cell expansion, which is driven by outward-directed turgor pressure generated inside the cell. In return, changes in cell wall architecture need to be monitored by individual cells, and to be coordinated across cells in a growing tissue, for an organ to attain its regular size and shape. Cell wall surveillance also comes also into play in the reaction against certain stresses, including for example infection by plant pathogens, many of which break through the cell wall during infection, thereby generating wall-derived factors that can induce defense responses. There is only limited knowledge regarding the molecular system that monitors the composition and status of the cell wall. Here we provide further insight into the mechanism. We show that the cell surface receptor STRUBBELIG, previously known to control organ development in Arabidopsis, also promotes the cell's response to reduced amounts of cellulose, a main component of the cell wall.

Introduction

Cell-cell communication is essential to regulate cellular behavior during many processes, including growth, development, and stress responses. In plants, the extra-cellular cell wall constitutes a central element of the underlying molecular mechanisms. It is mainly composed of carbohydrates, such as cellulose, hemicellulose, and pectin, and phenolic compounds, including lignin. Moreover, the cell wall also contains a plethora of different cell-wall-bound proteins [1,2]. It

imposes restrictions on cell expansion and the movement of cells and serves as a barrier to pathogen attack. The cell wall counteracts turgor-driven growth and thus cell wall remodeling is required for cell expansion [3]. Cell wall fragments released by pathogen-derived lytic enzymes can act as danger signals and elicit plant immunity responses [4]. These observations imply a necessity for plant cells to monitor cell wall integrity (CWI). Such a mechanism would sense any physico-chemical alterations that occurred in the cell wall, and elicit a corresponding compensatory and protective cellular response [5–7].

Little is known about the molecular mechanisms that reside at the nexus of monitoring the cell wall status and the control of development and stress responses. Only a few cell surface signaling factors are presently implicated in monitoring CWI [5–7]. For example, a complex between RECEPTOR-LIKE PROTEIN44 (RLP44) and BRASSINOSTEROID INSENSITIVE1 (BRI1), the brassinosteroid receptor, specifically connects BRI1-mediated signaling to the detection of pectin modifications [8,9]. The extracellular domain of FERONIA (FER), a member of the *Catharanthus roseus* Receptor-like Kinase1-like (CrRLK1L) family of receptor kinases (RKs) originally identified on the basis of its role in sexual reproduction [10], binds pectin in vitro. *FER* is also required to prevent cell bursting upon exposure of root cells to salt [11]. Signaling mediated by ANXUR1 (ANX1) and ANX2, two other members of the CrRLK1L family, appears to contribute to monitoring cell wall integrity and the prevention of the premature burst of pollen tubes [12–15].

Plant cells also respond to changes in cellulose levels in the cell wall. Cellulose is present in the form of microfibrils that constitute the main load-bearing elements

103 resisting turgor pressure. The microfibrils are embedded in matrix polysaccharides,
104 mainly various hemicelluloses and pectins [1,2]. Cellulose is synthesized by cellulose
105 synthase (CESA) complexes at the plasma membrane (PM) [16]. The effects of a
106 reduced production of cellulose on plant growth and development can be studied by
107 analyzing mutants with defects in genes encoding CESA subunits involved in primary
108 cell wall biosynthesis [17–21]. Alternatively, pharmacological approaches can be
109 applied. The herbicide isoxaben is a well-characterized inhibitor of cellulose
110 biosynthesis [22,23]. A number of findings suggest CESAs to be the direct targets of
111 isoxaben. First, several known isoxaben-resistant mutants carry mutations near the
112 carboxyl terminus of certain CESA subunits [24,25]. Second, isoxaben induces a
113 rapid clearing of CESA complexes from the PM [26]. Third, isoxaben uptake or
114 detoxification appears unaffected in resistant plants [27].
115
116 The reaction of liquid culture-grown seedlings to isoxaben-induced cellulose
117 biosynthesis inhibition (CBI) represents a thoroughly studied stress response to cell
118 wall damage (CWD) [28–31]. The response is sensitive to osmotic support and
119 eventually includes the upregulation of stress response genes, the production of
120 reactive oxygen species (ROS), an accumulation of phytohormones, such as jasmonic
121 acid (JA), changes in cell wall composition, including the production of ectopic lignin
122 and callose, and finally growth arrest. Similar effects were also observed when
123 studying the phenotypes of different *cesA* mutants [17–21].
124
125 The mechanism controlling the CWD response to CBI is known to involve three RKs
126 [28]. THESEUS1 (THE1), another member of the CrRLK1L family, was first
127 implicated in this process [32]. *THE1* was identified based on its genetic interaction

with *PROCUSTE1* (*PRC1*), a gene encoding a CESA6 subunit [21]. Amongst others, cellulose-deficient *prc1* single mutants exhibit reduced hypocotyl length and ectopic lignin accumulation. In *the1 prc1* double mutants these effects are ameliorated although cellulose levels remain reduced [32]. Moreover, *THE1* is required for the altered expression levels of several stress-response genes upon exposing liquid-grown seedlings to isoxaben [33]. Recently, the leucine-rich repeat (LRR)-XIIb family RK MALE DISCOVERER1-INTERACTING RECEPTOR LIKE KINASE 2/LEUCINE-RICH REPEAT KINASE FAMILY PROTEIN INDUCED BY SALT STRESS (MIK2/LRR-KISS) [34,35] and the LRR-XIII family member FEI2 [36] have also been shown to participate in the isoxaben-induced cell wall stress response [28,33,37]. Genetic analysis revealed that *THE1* and *MIK2* have overlapping but also distinct functions, suggesting a complex regulation of the CBI response, with *THE1* and *MIK2* promoting this response via different mechanisms. *FEI2* appears to be part of the *THE1* genetic pathway [28].

Tissue morphogenesis in Arabidopsis requires signaling mediated by the atypical LRR-RK STRUBBELIG (SUB). SUB, also known as SCRAMBLED (SCM), is a member of the LRR-V family of RKs and controls several developmental processes, including floral morphogenesis, integument outgrowth, leaf development and root hair patterning [38–40]. SUB represents an atypical receptor kinase, as its *in vivo* function does not require enzymatic activity of its kinase domain [38,41]. Our previous studies indicate that SUB not only localizes to the PM but is also present at plasmodesmata (PD), channels interconnecting most plant cells [42,43], where it physically interacts with the PD-specific C2 domain protein QUIRKY (QKY) [44].

Current data also associate *SUB* signaling to cell wall biology. For example, whole-genome transcriptomics analysis revealed that many genes responsive to *SUB*-mediated signal transduction relate to cell wall remodeling [45]. Moreover, Fourier-transform infrared spectroscopy (FTIR)-analysis indicated that flowers of *sub* and *qky* mutants share overlapping defects in cell wall biochemistry [46]. Thus, apart from functionally connecting RK-mediated signal transduction and PD-dependent cell-cell communication *SUB* signaling also relates to cell wall biology.

Here, we report on a further exploration of the connection between the cell wall and SUB function. Our data reveal a novel role for *SUB* signaling in the CBI-induced CWD response. We show that *SUB* affects several processes, such as ROS accumulation, stress gene induction as well as ectopic lignin and callose accumulation, that are initiated upon application of exogenous isoxaben. Moreover, *SUB* signaling is necessary for maintaining cell shape and recovery of root growth after transient exposure to isoxaben. Our genetic data further indicate that *SUB*, *THE1*, and *MIK2* act in different pathways and that not all contributions of *SUB* to CBI-induced CWD signaling require *QKY* function.

Results

In light of the connection between SUB signaling and cell wall biology, we set out to address if *SUB* plays a role in the seedling responses to cell wall stress. In particular, we focused on the possible role of *SUB* in the isoxaben-induced CWD response.

SUB does not affect cellulose production

We first investigated if *SUB* influences cellulose biosynthesis in seven days-old seedlings. We first analyzed transcript levels of *CESA1*, *CESA3*, and *CESA6* in wild-type and *sub*. The three genes encode the CESA isoforms present in CSCs of the primary cell wall [47,48]. We could not detect differences in transcript levels of *CESA1*, *CESA3*, and *CESA6* between *sub* and wild-type in quantitative real-time polymerase chain reaction (qPCR) experiments (Fig. 1A). Moreover, we assessed the levels of cellulose and failed to detect differences between *sub* and wild-type (Fig. 1B). We could however detect a reduction in cellulose levels in *prc1-1* that was comparable to previous findings [21] (Fig. 1B). The results indicate that *SUB* does not play a central role in cellulose biosynthesis in seedlings.

SUB affects the isoxaben-induced CWD response

We then assessed if *SUB* activity is necessary for accumulation of reactive oxygen species (ROS) in response to isoxaben-induced CWD. To this end we exposed seven-day wild-type and *sub-9* seedlings, grown on half-strength Murashige and Skoog (MS) plates containing one percent sucrose, to 600 nM isoxaben in a time-course experiment. Seedlings were monitored for up to 120 minutes, at 30 minutes intervals. Upon treatment we assessed fluorescence intensity of the intracellular ROS probe H_2DCFDA in roots [49,50]. In wild-type Col-0 seedlings treated for 30 minutes with isoxaben, we noticed an increase in H_2DCFDA signal compared with untreated seedlings (Fig. 2A,B). Signal intensity of the probe increased further in seedlings exposed for 60 minutes. This signal intensity remained for up to 120 minutes of continuous exposure to isoxaben. In *sub-9* seedlings we detected a slightly increased H_2DCFDA signal after 60 minutes (Fig. 2A,C). However, signal intensity was noticeably reduced in comparison to wild type. In comparison to the mock control,

202 isoxaben-treated *sub-9* seedlings continued to show an enhanced signal intensity for
203 up to 120 minutes of exposure, although the relative difference to signal levels of
204 mock-treated seedlings was never as pronounced as in wild type. Thus in comparison
205 to wild type, *sub-9* mutants showed a delayed onset of H_2CDFDA signal appearance
206 and an overall reduced signal intensity for the time frame analyzed. The results
207 indicate that isoxaben causes the formation of intracellular ROS in roots of treated
208 wild-type seedlings within 30 minutes of application. Moreover, *SUB* affects this
209 ROS response.
210
211 Next, we tested if *SUB* activity is required for the transcriptional regulation of several
212 marker genes, known to respond to isoxaben-induced CWD within eight hours [31].
213 We performed quantitative real-time polymerase chain reaction (qPCR) experiments
214 using RNA isolated from seven days-old liquid-grown seedlings that had been
215 incubated with 600 nM isoxaben for eight hours. We observed that isoxaben-induced
216 upregulation of *CCR1*, *CCR2*, *PDF1.2*, and *TCH4* was attenuated in *sub-9* mutants
217 compared to wild type (Fig. 2D). We did not detect a significant alteration in the
218 upregulation of other tested marker genes, including *VSP1*, *FRK1*, *CYP81F2*, *TIP2;3*,
219 and *RBOHD*, in *sub-9* seedlings. In wild type, upregulation of *CCR1* and *PDF1.2*
220 expression was already detected upon four hours of isoxaben treatment [31]. We
221 observed that expression levels of the two genes were significantly reduced in *sub-9*
222 upon a four-hour exposure to isoxaben (Fig S1). These results indicate that *SUB* is
223 required for the isoxaben-induced upregulation of expression of several marker genes.
224
225 The seedlings' response to isoxaben also includes the accumulation of the
226 phytohormone JA [31]. We thus tested if *SUB* affects the isoxaben-induced

227 production of JA in seven days-old liquid-grown seedlings that had been incubated in
228 600 nM isoxaben for seven hours. We found that JA accumulation appeared largely
229 unaffected in *sub-9* or *sub-21* mutants while the two overexpressing lines showed
230 strongly diminished JA levels following isoxaben treatment (Fig. 2E). The results
231 indicate that *SUB* is not required for isoxaben-induced JA accumulation. The
232 observation that the phenotypes of the loss-of-function and overexpressing mutants
233 are not easy to reconcile with each other renders an interpretation of the effects seen
234 in the *SUB* overexpressing lines difficult. Thus, their biological relevance needs to be
235 assessed in further experiments.
236
237 Isoxaben-induced CBI eventually results in the alteration of cell wall biochemistry as
238 evidenced by the ectopic accumulation of lignin and callose [31]. To investigate if
239 *SUB* affects lignin biosynthesis, we estimated lignin accumulation in roots using
240 phloroglucinol staining after exposing six-day-old liquid-grown seedlings to 600 nM
241 isoxaben for 12 hours. We observed reduced phloroglucinol staining in the root
242 elongation zone of *sub-1* seedlings in comparison to wild type L*er* indicating less
243 ectopic lignin production (Fig. 3A,B). We also noticed reduced phloroglucinol signal
244 in *sub-9* seedlings (Col-0 background) although the effect was less prominent.
245 However, in our hands Col-0 wild-type plants exhibited an overall weaker
246 phloroglucinol staining indicating that isoxaben-induced lignin accumulation does not
247 occur to the same level as in L*er* (Fig. 3A,B). We could detect increased
248 phloroglucinol staining in two out of three *pUBQ::SUB:mCherry* lines (L1, O3) (Fig.
249 3A,B).
250

Isoxaben-treatment for 24 hours results in the formation of callose in cotyledons of wild-type seedlings [31]. Thus, we tested if *SUB* is required for this process as well. To this end we transferred seven days-old plate-grown seedlings to liquid medium without isoxaben for 12 hours. Subsequently, medium was exchanged, and seedlings were kept in 600 nM isoxaben for another 24 hours followed by callose detection using aniline blue staining [51]. As expected, we observed prominent aniline blue staining in cotyledons of L*er* and Col wild-type seedlings upon isoxaben treatment (Fig. 3C,D). By contrast, we detected strongly reduced aniline blue staining in cotyledons of isoxaben-treated *sub-1* and *sub-4* (both in L*er*) as well as *sub-9* and *sub-21* (both in Col). In contrast, and similar to the phloroglucinol staining described above, we detected stronger aniline blue staining in *SUB* overexpressors (lines L1, O3) (Fig. 3C,D).

Taken together, the results indicate that *SUB* is required for the isoxaben-induced formation of lignin and callose in seedlings.

The *SUB*-mediated CBI response is sensitive to sorbitol

The isoxaben-induced CWD response is sensitive to turgor pressure, as indicated by the suppression of lignin or callose accumulation in the presence of osmotica, such as sorbitol [28,30,31]. To test if *SUB* affects a turgor-sensitive CBI response we compared isoxaben-induced accumulation of lignin and callose in six days-old Col-0, *sub-9,* and *pUBQ::SUB:mCherry* seedlings in co-treatments with 600 nM isoxaben and 300 mM sorbitol (Fig. 4A-C). We observed that sorbitol suppressed lignin and callose accumulation in all tested genotypes, including SUB:mCherry overexpressing lines, which show hyperaccumulation of lignin or callose in the absence of sorbitol.

276

277 ***SUB* attenuates isoxaben-induced cell swelling and facilitates root growth**

278 **recovery**

279 Next, we assessed the biological relevance of *SUB* in the isoxaben-induced CWD

280 response. Exposure of seedlings to isoxaben eventually results in the shortening and

281 swelling of cells of the root epidermis, possibly a result of reduced microfibril

282 formation in the cell wall [28]. We transferred six days-old plate-grown seedlings into

283 a mock solution or a solution containing 600 nM isoxaben for up to seven hours. We

284 then assessed the timing of the initial appearance of altered cellular morphology of

285 root epidermal cells. In addition, we monitored the severity of the phenotype. We

286 focused on cells of the elongation zone that bordered the root meristem. Notably, we

287 did not observe any obvious morphological alterations in mock-treated wild-type or

288 mutant seedlings (Fig. 5). In Col-0 wild-type seedlings cell shortening and swelling

289 first became noticeable during the five to six-hour interval proceeding treatment (Fig.

290 5) (44/96 seedlings total, n = 4), as reported previously [28]. Upon isoxaben

291 application to *sub-9* or *sub-21* seedlings, however, similar cellular alterations were

292 already detected at the three to four-hour interval post treatment initiation (*sub-9*:

293 23/57, n = 2; *sub-21*: 20/46, n = 2). In addition, *sub* mutants exhibited more

294 pronounced cellular alterations after seven hours of isoxaben treatment in comparison

295 to wild type (Fig. 5).

296

297 In wild-type seedlings, a 24-hour exposure to isoxaben results in a temporary stop of

298 root growth followed by a rapid recovery [28]. We tested the role of *SUB* in root

299 growth recovery upon a 24 hour-treatment with isoxaben. Six-day-old wild-type and

300 mutant seedlings grown on plates were transferred onto media containing 600 nM

isoxaben for 24 hours, then moved to fresh plates lacking isoxaben. Seedlings were then monitored for continued root growth at 24 hour intervals, for a total of 72 hours (Table 1). As control, we used the *ixr2-1* mutant, which is resistant to isoxaben due to a mutation in the *CESA6* gene [24,25,52]. We observed that 98 percent of *ixr2-1* seedlings recovered root growth already within 24 hours, indicating that treatment did not generally impact the seedlings' ability to recover root growth. We then tested wild-type seedlings. We noticed that 46 percent of L*er* and 39 percent of Col seedlings had resumed root growth after 24 hours. By 72 hours, 86 percent of L*er* and 90 percent of Col seedlings had recovered root growth. In contrast, a significantly reduced fraction of *sub-1* and *sub-4* mutants had resumed root growth when compared to wild-type L*er* (Table 1). The *sub-9* and *sub-21* mutants also showed reduced root growth recovery in comparison to Col although *sub-21* appeared less affected than *sub-9*. Importantly, *ixr2-1 sub-9* mutants behaved identical to *ixr2-1* single mutants at all time points scored. These findings indicate that *ixr2-1* is epistatic to *sub-9* and that the observed isoxaben-induced decrease in root growth recovery in *sub-9* mutants relates to the herbicide.

Taken together, the results suggest that *sub* mutants are hypersensitive to isoxaben treatment and that *SUB* facilitates root growth recovery, and represses cell size and shape changes in root epidermal cells during the isoxaben-induced CWD response.

SUB attenuates root growth in _prc1-1_

PRC1 encodes the CESA6 subunit of cellulose synthase [21] and *prc1* loss-of-function mutants show reduced cellulose levels [21] (Fig. 1B). In addition, *prc1-1* mutants are characterized by a reduced elongation of etiolated hypocotyls and roots

326 [21]. To test if *SUB* also affects a biological process in a scenario where cellulose
327 reduction is induced genetically we compared root length in *sub-9*, *sub-21*, and *prc1-1*
328 single and *sub-9 prc1-1* double mutants (Fig. 6A,B). We found that root length of
329 *sub-9* or *sub-21* did not deviate from wild type while root length of *prc1-1* was
330 markedly smaller in comparison to wild type, confirming previous results [21].
331 Interestingly, however, we observed that *sub-9 prc1-1* exhibited a significantly longer
332 root than *prc1-1* though *sub-9 prc1-1* roots were still notably smaller than wild type
333 roots. The results indicate that *SUB* contributes to root growth inhibition in *prc1-1*.
334
335 **_SUB_ and _QKY_ contribute differently to the CBI response**
336 Evidence suggests that a protein complex including SUB and QKY is important for
337 SUB-mediated signal transduction regulating tissue morphogenesis [44,53,54]. Thus,
338 we wanted to explore if *QKY* is also required for the isoxaben-induced CWD response
339 in seedlings. We first investigated if *QKY* affects the early isoxaben-induced changes
340 in intracellular ROS levels by assessing H_2CDFDA fluorescence in root tips of *qky-11*
341 seedlings that were treated with 600 nM isoxaben. We did not observe a difference in
342 signal intensity between mock and isoxaben-treated *qky-11* (Fig. 7A). Moreover,
343 signal intensity was similar to wild type (Fig. 2B) indicating that *QKY* does not
344 contribute to altered intracellular ROS levels in root tips of treated seedlings in a
345 noticeable fashion. We then tested if *QKY* promotes isoxaben-induced marker gene
346 expression in liquid-grown seedlings. Using qPCR we observed that *SUB* and *QKY*
347 affect a similar set of marker genes (Fig. 7B). Next, we assessed isoxaben-induced
348 lignin accumulation in wild-type and *qky* seedlings by phloroglucinol staining. We
349 noticed reduced staining in *qky-8* and *qky-11* mutants compared to wild type (Fig.
350 7C,D). Again, the effect was less obvious in Col-0. In addition, we noticed that *qky-*

351 *11* did not affect the absence of lignin accumulation in seedlings simultaneously
352 treated with isoxaben and sorbitol (Fig. 4A). We also investigated the role of *QKY* in
353 isoxaben-induced callose deposition by scoring the aniline blue-derived signal in
354 cotyledons. In contrast to *sub* mutants, however, we did not observe a significant
355 difference in signal strength between *qky-8*, *qky-11*, and wild type (Fig. 7E,F).
356 Regarding isoxaben-induced JA accumulation we found that *qky-11* seedlings did not
357 noticeable deviate from *sub* (Fig. 2E). We also analyzed isoxaben-induced shortening
358 and swelling of root epidermal cells in *qky-11* mutants (Fig. 4). We noticed the first
359 defects in a four to five hour interval and thus about an hour later than in *sub* mutants
360 (37/63, n = 3). Cell swelling after seven hours exposure to isoxaben was prominent in
361 *qky-11* but less severe in comparison to *sub-9* (Fig. 4). Finally, we investigated root
362 growth recovery after transient isoxaben application. We observed that *qky-8* and *qky-*
363 *11* mutants did not significantly deviate from wild type (Table 1).
364
365 Taken together, the results indicate that *QKY* and *SUB* contribute to the isoxaben-
366 mediated induction of an overlapping set of marker genes as well as to lignin
367 accumulation. Moreover, *QKY* also plays a role in the suppression of isoxaben-
368 induced alterations in cell morphology in the root epidermis. However, the results also
369 imply that *QKY* is not required for isoxaben-induced early ROS accumulation in root
370 tips as well as callose accumulation in cotyledons and does not affect root growth
371 recovery after transient exposure to isoxaben.
372
373 **_SUB_ and _THE1_ share partially overlapping functions**
374 *THE1* is a central regulator of the isoxaben-induced CBI response [28,33,37]. Our
375 data indicate that *SUB* and *THE1* have overlapping but also distinct functions in this

process. For example, *SUB* and *THE1* control isoxaben-induced lignin accumulation in roots (Fig. 3) [28,33]. However, in contrast to *THE1*, *SUB* was not shown to affect *FRK1* induction by isoxaben (Fig. 2D) [33]. We also found that root growth recovery of *the1-1* seedlings upon transient exposure to isoxaben did not deviate from wild type (Table 1). Moreover, we failed to detect an effect of *THE1* on root growth inhibition in *prc1-1*, while *SUB* contributes to this process (Fig. 6). We therefore explored further the relationship between *THE1* and *SUB*.

THE1 contributes to the reduction of hypocotyl length of cellulose-diminished *prc1-1* seedlings grown in the dark as evidenced by the partial recovery of hypocotyl elongation in *the1 prc1* double mutants [32]. We compared *sub-9 prc1-1* to *the1-1 prc1-1* with respect to hypocotyl elongation in six-day-old etiolated seedlings and root length in seven-day-old light-grown seedlings (Fig. 8). We observed strongly reduced hypocotyl elongation in *prc1-1* in comparison to wild type and a significant suppression of this reduction in *the1-1 prc1-1* double mutants (Fig. 8A,B), as described earlier [32]. In contrast, hypocotyl length in *sub-9* mutants was not decreased, nor was there a partial reversal of reduced hypocotyl elongation in *sub-9 prc1-1* double mutants (Fig. 8A,B). The results indicate that *SUB* does not affect hypocotyl elongation in etiolated wild-type or *prc1-1* seedlings.

Finally, we assessed the role of *THE1* in isoxaben-induced early ROS accumulation in root tips. We noticed no difference in H_2CDFDA signal intensity when comparing *the1-1* seedlings that had been treated with either mock or isoxaben for 30 minutes (Fig. 8C). By contrast, isoxaben-induced reporter signal in the root tip became stronger than the mock-mediated signal at the 60 minutes time point (Fig. 8C).

Overall the results resemble the findings obtained with *sub-9* mutants (Fig. 2C) although the response may be slightly less affected in *the1-1* in comparison to *sub-9*.

In summary, *SUB* and *THE1* are required for ROS and lignin accumulation in roots and show partial overlap with respect to stress marker gene induction. *SUB* and *THE1* show opposite effects on growth inhibition of roots and hypocotyls in *prc1* mutants and their functions differ with respect to root growth recovery.

Discussion

Cell wall signaling during plant development and stress responses relies on complex and largely unknown signaling circuitry [5–7,29,55]. Only a few RKs, including THE1, MIK2, and FEI2, have so far been shown to play a major role in CBI-induced CWD signaling [28,32,33,37]. Our data establish *SUB* signal transduction as a novel component in the molecular framework mediating the CWD response.

To date, published evidence has attributed a developmental role to *SUB*, particularly in the control of tissue morphogenesis and root hair pattern formation [38–40,45,56]. The evidence provided in this work identifies a novel role for *SUB* in CWD signaling. Application of isoxaben results in reduced levels of cellulose [22,23]. Our results indicate that *SUB* affects multiple aspects of the isoxaben-induced CWD response. The observation that *sub-9* partially suppresses reduced root length exhibited by *prc1-1* indicates that *SUB* also mediates a CWD response that is caused by a genetic reduction in cellulose content. Thus, the collective data support the notion that the origin of the CWD relates to the reduced production of cellulose, a major

425 carbohydrate component of the cell wall, and that *SUB* contributes to the
426 compensatory cellular response to this type of cell-wall-related stress.
427
428 The data indicate that *SUB* already affects the early response to isoxaben-induced
429 CWD, in particular ROS production. Previous results had revealed that the isoxaben-
430 induced CWD response involves *THE1*-dependent ROS production [31,57]. In
431 luminol-based extracellular ROS assays involving entire seedlings ROS production
432 could be detected after around three to four hours following the application of
433 isoxaben [57]. We used the intracellular ROS probe H_2CDFDA and a microscope-
434 based method that enabled tissue-level resolution. H_2CDFDA has for example been
435 used to assess basal intracellular ROS levels when studying *GLYCERALDEHYDE-3-*
436 *PHOSPHATE DEHYDROGENASE* (*GAPDH*) genes and root hairs [49,50]. Our time-
437 course data indicate that isoxaben induces the formation of intracellular ROS in the
438 root meristem within 30 minutes. To our knowledge the isoxaben-dependent change
439 in H_2CDFDA fluorescence signal represents the earliest available marker for the
440 isoxaben-induced CWD response. It also indicates that this response occurs much
441 earlier than previously appreciated.
442
443 The results suggest that *SUB* is required for full induction of several marker genes,
444 such as *CCR1*, *PDF1.2*, or *TCH4*. Moreover, the data indicate that *SUB* promotes
445 CBI-induced accumulation of lignin and callose. In addition, *SUB* does not obviously
446 influence the reduced lignin and callose state the results from double application of
447 sorbitol and isoxaben. This result indicates that *SUB* mediates an osmosensitive CWD
448 response. It has been proposed that a mechanical stimulus initiates the CWD response
449 with the reduction in cellulose and corresponding weakening of the cellulose

framework counteracting turgor pressure. In this model, a displacement or distortion of the plasma membrane relative to the cell wall could take place [28,58–61]. We speculate that *SUB* signaling likely involves as yet unknown mechano-sensitive factors. The combined results fulfil the criteria that have been established for a CBI-induced CWD response [28,31].

Interestingly, different loss-of-function (*sub-1*, *sub-9*, *sub-21*) or gain-of-function (*pUBQ::SUB:mCherry*) mutants show reciprocal effects regarding lignin and callose accumulation, with *sub* mutants showing less and several independent *pUBQ::SUB:mCherry* lines exhibiting higher levels of lignin or callose, respectively, upon application of isoxaben. Based on this evidence, we propose the model that *SUB* represents an important genetic regulator of isoxaben-induced lignin and callose accumulation and thus cell wall composition.

Several lines of evidence indicate that *SUB* plays a biologically relevant role in CWD signaling initiated by a reduction in cellulose content. Firstly, *SUB* attenuates isoxaben-induced cell bulging in the epidermal cells of the meristem-transition zone boundary of the root. Secondly, *SUB* facilitates root growth recovery upon transient exposure of seedlings to isoxaben. Thirdly, *SUB* is involved in root growth inhibition that is a consequence of a genetic reduction of cellulose content. In particular, root length of *sub-9 prc1-1* double mutant seedlings is less diminished in comparison to the root length of *prc1-1* single mutant seedlings. The results imply that *SUB* contributes to a compensatory response that counteracts the cellular and growth defects caused by reduced cellulose synthesis and further support the notion that *SUB* plays a central role in CBI-induced CWD signaling.

How does SUB relate to other known RK genes mediating the response to CBI-induced cell wall stress, such as *THE1* and *MIK2*? *SUB*, *THE1*, and *MIK2* all promote isoxaben-induced ectopic lignin production. The three genes are also required for full induction of certain stress marker genes. However, while *THE1* and *MIK2* control *FRK1* expression, and *MIK2* also affects the expression of *CYP81F2* [33], our data indicate that *SUB* is not required for the induction of these two genes. In addition, *THE1* and *MIK2* are necessary for isoxaben-induced JA accumulation [28,33,57], a process that apparently does not require *SUB* function. We also did not observe an effect of *THE1* on root growth recovery upon transient exposure to isoxaben. In addition, we did not find an altered hypocotyl length of *sub-9 prc1-1* in comparison to *the1-1* indicating that *SUB* does not affect hypocotyl growth inhibition in etiolated *prc1-1* seedlings, in contrast to *THE1* [32]. At the same time, our data suggest that *SUB* contributes to root growth inhibition in *prc1-1*. However, our evidence does not support a function for *THE1* in this process, as root length of *the1-1 prc1-1* double mutants did not deviate from the root length observed for *prc1-1* single mutants. This finding also implies that the lignin accumulation in the mature root parts of *prc1-1* (suppressed in *prc1-1 the1-1* double mutants) [32] does not correlate with root growth inhibition. Finally, we did not observe the left-hand root skewing in *sub* seedlings that is characteristic for *mik2* mutants [33], and we failed to observe floral defects in *mik2* or *the1* mutants. Taken together, the data suggest that *SUB* has both overlapping and distinct functions with *THE1* and *MIK2*. As the most parsimonious explanation of our results, we propose that *SUB* contributes to CBI-induced cell wall damage signaling independently from *THE1* and *MIK2* signaling, however the signaling pathways

499 downstream of the different cell surface receptor kinases eventually partially converge
500 and contribute to a subset of overlapping downstream responses.
501
502 *QKY* represents a central genetic component of *SUB*-mediated signal transduction
503 during tissue morphogenesis and root hair patterning [45]. The expression pattern of
504 *QKY* and *SUB* fully overlap [44] and present evidence supports the notion that SUB
505 and QKY are part of a protein complex with QKY likely acting upstream to, or in
506 parallel with, SUB [44,53,54]. However, genetic and whole-genome transcriptomic
507 data suggested that *SUB* and *QKY* also play distinct roles during floral development
508 [45]. The data presented in this study reveal that *SUB* and *QKY* both contribute to
509 CBI-induced CWD signaling. Similar to *SUB QKY* is required for full induction of the
510 same marker genes and for lignin accumulation. Moreover, *QKY* is also necessary for
511 the prevention of cell bulging in the epidermal cells of the meristem-transition zone
512 boundary of the root although the weaker phenotype of *qky-11* mutants indicates a
513 lesser requirement for *QKY* in comparison to *SUB*. However, our data also indicate
514 that *QKY* is not required for early ROS accumulation, ectopic callose accumulation,
515 and root growth recovery as we found these three processes to be not noticeably
516 affected in *qky* mutants. Thus, these data provide genetic evidence that the functions
517 of *SUB* and *QKY* do not completely overlap and that *SUB* exerts CWD signaling
518 functions that are independent of *QKY*. One way to rationalize these findings is to
519 assume that SUB can also function in isolation or in protein complexes or pathways
520 that do not involve QKY.
521
522 The diverse functions of *SUB* in development and the CWD response are likely to be
523 achieved through participation in different signaling pathways. It is not uncommon

that RKs play important roles in several biological processes. In this respect, SUB resembles for example the RK BRASSINOSTEROID INSENSITIVE 1-ASSOCIATED KINASE 1 (BAK1) / SOMATIC EMBROYGENESIS RECEPTOR KINASE 3 (SERK3), which functions in growth, development, and plant defense [62,63]. BAK1 interacts with a range of different LRR-RKs, including FLAGELLIN SENSING 2 (FL2) and BRASSINOSTEROID INSENSITIVE 1 (BRI1), and the discrimination between the growth and immunity functions of BAK1 was recently shown to rely on phosphorylation-dependent regulation [64,65]. In light of these considerations it is reasonable to propose that SUB is a member of different receptor complexes. As kinase activity of SUB is not required for its function [38] SUB could act as a scaffold around which the components of the various complexes assemble. A scaffold role has for example been proposed for the RK AtCERK1/OsCERK1 in chitin signaling or the RK FER in immune signaling [66,67]. It will be interesting to explore this notion in future work.

Materials and Methods

Plant work, plant genetics and plant transformation

Arabidopsis thaliana (L.) Heynh. var. Columbia (Col-0) and var. Landsberg (*erecta* mutant) (L*er*) were used as wild-type strains. Plants were grown as described earlier [45]. The *sub-1*, *qky-8* (all in Ler), and the *sub-9* and *qky-11* mutants (Col) have been characterized previously [38,41,44,45]. The *prc1-1* [21], *the1-1* [32], and *ixr2-1* [24] alleles were also described previously. The *sub-21* (Col) allele was generated using a CRISPR/Cas9 system in which the egg cell-specific promoter pEC1.2 controls Cas9 expression [68]. The single guide RNA (sgRNA) 5'-

549 TAATAACTTGTATATCAACTT-3' binds to the region +478 to +499 of the *SUB*
550 coding sequence. The sgRNA was designed according to the guidelines outlined in
551 [69]. The mutant carries a frameshift mutation at position 495 relative to the *SUB* start
552 AUG, which was verified by sequencing. The resulting predicted short SUB protein
553 comprises 67 amino acids. The first 39 amino acids correspond to SUB and include its
554 predicted signal peptide of 29 residues, while amino acids 40 to 67 represent an
555 aberrant amino acid sequence. The pUBQ::gSUB:mCherry plasmid used to generate
556 the *SUB* overexpression lines L1 and O3 was generated previously [44]. Wild-type,
557 and *sub* mutant plants were transformed with different constructs using
558 Agrobacterium strain GV3101/pMP90 [70] and the floral dip method [71]. Transgenic
559 T1 plants were selected on Kanamycin (50 µg/ml), Hygromycin (20 µg/ml) or
560 Glufosinate (Basta) (10 µg/ml) plates and transferred to soil for further inspection.
561
562 **Cellulose quantification**
563 Seedlings were grown on square plates with half strength MS medium and 0.3%
564 sucrose supplemented with 0.9% agar for seven days. Cellulose content was measured
565 following the Updegraff method essentially as described [72,73], with minor
566 modifications as outlined here. Following the acetic nitric treatment described in [72],
567 samples were allowed to cool at room temperature and transferred into 2 ml
568 Eppendorf safety lock tubes. Samples were then centrifuged at 14000 rpm at 15°C for
569 15 min. The acetic nitric reagent was removed carefully without disturbing the
570 pelleted material at the bottom of the tube. 1 ml of double-distilled H_2O was added,
571 and the sample was left on the bench for 10 min at room temperature followed by
572 centrifugation at 14000 rpm at 15°C for 15 min. After aspirating off the H_2O 1 ml
573 acetone was added and the samples were incubated for another 15 min, followed by

574 centrifugation at 14000 rpm at 15°C for 15 min. Afterwards acetone was removed,
575 and samples were air-dried overnight. Then the protocol was continued as described
576 in [72].
577
578 **PCR-based gene expression analysis**
579 For quantitative real-time PCR (qPCR) of *CesA* and stress marker genes 35 to 40
580 seedlings per flask were grown in liquid culture under continuous light at 18°C for
581 seven days followed by treatment with mock or 600 nM isoxaben for eight hours or
582 on plates (21°C, long-day conditions). With minor changes, RNA extraction and
583 quality control were performed as described previously [74]. cDNA synthesis, qPCR,
584 and analysis were done essentially as described [75]. Primers are listed in
585 Supplemental Table 1.
586
587 **ROS, lignin, and callose staining**
588 Intracellular ROS accumulation in root meristems was estimated using the H_2DCFDA
589 fluorescent stain essentially as described [50]. Seeds were grown on square plates
590 with half strength MS medium and 1% sucrose supplemented with 0.9% agar. The
591 seeds were stratified for two days at 4˚C and incubated for seven days at 22˚C under
592 long day conditions, at a 10 degree inclined position. Seven days-old seedlings were
593 first transferred into multi-well plates containing half strength liquid MS medium
594 supplemented with 1% sucrose for two hours. Then medium was exchanged with
595 liquid medium containing either DMSO (mock) or 600nM isoxaben without
596 disturbing seedlings. 10 min prior to each time point seedlings were put in the dark
597 and the liquid medium was supplemented with 100 µM H_2DCFDA staining solution.
598 Images was acquired with a confocal microscope. For quantification a defined region

of interest (ROI) located 500 µm above the root tip (excluding the root cap) was used in all samples. Staining for lignin (phloroglucinol) and callose (aniline blue) was performed as described in [33] and [51], respectively. ROS, phloroglucinol and aniline blue staining was quantified on micrographs using ImageJ software [76].

JA measurements

Chemicals

Jasmonic acid-d_0 and jasmonic acid-d_5 were obtained from Santa Cruz Biotechnology, Inc. (Dallas, TX, USA). Formic acid was obtained from Merck (Darmstadt, Germany), ethyl acetate and acetonitrile (LC-MS grade) were obtained from Honeywell (Seelze, Germany). Water used for chromatographic separations was purified with an AQUA-Lab – B30 – Integrity system (AQUA-Lab, Ransbach-Baubach, Germany).

Sample preparation

Approximately 35 to 40 seedlings per flask were grown in liquid culture (1/2 MS, 0.3% sucrose) under continuous light and 18°C for seven days followed by treatment with mock or 600 nM isoxaben for seven hours and harvesting in liquid nitrogen. The grinded plant material (100-200 mg) was placed in a 2 mL bead beater tube (CKMix-2 mL, Bertin Technologies, Montigny-le-Bretonneux, France), filled with ceramic balls (zirconium oxide; mix beads of 1.4 mm and 2.8 mm), and an aliquot (20 μL) of a solution of acetonitrile containing the internal standard (-)*trans*-jasmonic acid-d_5 (25 μg/mL), was added. After incubation for 30 min at room temperature, the tube was filled with ice-cold ethyl acetate (1 mL). After extractive grinding (3 × 20 s with 40 s breaks; 6000 rpm) using the bead beater (Precellys Homogenizer, Bertin

624 Technologies, Montigny-le-Bretonneux, France), the supernatant was membrane
625 filtered (0.45 μm), evaporated to dryness (Christ RVC 2-25 CD *plus*, Martin Christ
626 Gefriertrocknungsanlagen GmbH, Osterode am Harz, Germany), resolved in
627 acetonitrile (70 μL) and injected into the LC−MS/MS-system (2 μL).
628
629 *Liquid Chromatography-Triple Quadrupole Mass Spectrometry (LC−MS/MS)*
630 Phytohormone concentrations were measured by means of UHPLC-MS/MS using a
631 QTRAP 6500+ mass spectrometer (Sciex, Darmstadt, Germany) in the multiple
632 reaction monitoring (MRM) mode. Positive ions were detected at an ion spray voltage
633 at 5500 V (ESI+) and the following ion source parameters: temperature (550°C), gas
634 1 (55 psi), gas 2 (65 psi), curtain gas (35 psi), entrance potential (10 V) and collision
635 activated dissociation (3 V). The temperature of the column oven was adjusted to
636 40°C. For plant hormone analysis, the MS/MS parameters of the compounds were
637 tuned to achieve fragmentation of the [M+H]+ molecular ions into specific product
638 ions: (-)trans-jasmonic acid-d_0 211→133 (quantifier) and 211→151 (qualifier),
639 (-)trans-jasmonic acid-d_5 216→155 (quantifier) and 216→173 (qualifier). For the
640 tuning of the mass spectrometer, solutions of the analyte and the labelled internal
641 standard (solved in acetonitrile:water, 1:1) were introduced into the MS system by
642 means of flow injection using a syringe pump. Separation of all samples was carried
643 out by means of an ExionLC UHPLC (Shimadzu Europa GmbH, Duisburg,
644 Germany), consisting of two LC pump systems (ExionLC AD), an ExionLC degasser,
645 an ExionLC AD autosampler, an ExionLC AC column oven – 240 V and an ExionLC
646 controller. After sample injection (2 μL), chromatography was carried out on an
647 analytical Kinetex F5 column (100 × 2.1 mm^2, 100 Å, 1.7 μm, Phenomenex,
648 Aschaffenburg, Germany). Chromatography was performed with a flow rate of 0.4

649 mL/min using 0.1% formic acid in water (v/v) as solvent A and 0.1% formic acid in
650 acetonitrile (v/v) as solvent B, and the following gradient: 0% B held for 2 min,
651 increased in 1 min to 30% B, in 12 min to 30% B, increased in 0.5 min to 100% B,
652 held 2 min isocratically at 100% B, decreased in 0.5 min to 0% B, held 3 min at 0%
653 B. Data acquisition and instrumental control was performed using Analyst 1.6.3
654 software (Sciex, Darmstadt, Germany).
655
656 **Hypocotyl and root measurements**
657 For measuring etiolated hypocotyl length, seedlings were grown for five days on half-
658 strength MS agar supplemented with 0.3 % sucrose. Seedlings were photographed and
659 hypocotyl length was measured using ImageJ. For root growth assays, seedlings were
660 grown for seven days in long-day conditions at 21°C on half-strength MS agar
661 supplemented with 0.3 % sucrose. Plates were inclined at 10 degrees. Root length was
662 measures using ImageJ. For root growth recovery assays seedlings were grown on
663 half-strength MS agar supplemented with 0.3 % sucrose. Seeds were stratified for two
664 days followed by incubation at 21°C in long day conditions for seven days. Plates
665 were inclined at 10 degrees. Individual seedlings were transferred to plates containing
666 either 0.01 percent DMSO (mock) or 600 nM isoxaben for 24 hours. After treatment,
667 seedlings were transferred onto half-strength MS agar plates supplemented with 0.3 %
668 sucrose. The position of the root tip was marked under a dissection microscope. Root
669 length was measured every 24 hours for up to three days. For root cell bulging assays
670 seedlings were grown for seven days in long-day conditions at 21°C on half-strength
671 MS agar supplemented with 0.3 % sucrose. Plates were inclined at 10 degrees.
672 Individual seedlings were first transferred into liquid medium for two hours
673 habituation followed by treatment with 600 nM isoxaben for up to seven hours. To

674 take images, seedlings were stained with 4 µM FM4-64 for 10 minutes and imaged
675 using confocal microscopy. Confocal micrographs were acquired at each time point.
676 All hypocotyl length or root measurements were performed in double-blind fashion.
677
678 **Statistics**
679 Statistical analysis was performed with PRISM8 software (GraphPad Software, San
680 Diego, USA).
681
682 **Microscopy and art work**
683 Images of seedlings exhibiting phloroglucinol staining were taken on a Leica MZ16
684 stereo microscope equipped with a Leica DFC320 digital camera. Images of
685 hypocotyl and root length were taken on a Leica SAPO stereo microscope equipped
686 with a Nikon Coolpix B500 camera. Aniline blue-stained cotyledons and root cell
687 bulging were imaged with an Olympus FV1000 setup using an inverted IX81 stand
688 and FluoView software (FV10-ASW version 01.04.00.09) (Olympus Europa GmbH,
689 Hamburg, Germany) equipped with a 10x objective (NA 0.3). For assessing cell
690 bulging a projection of a 5 µm z-stack encompassing seven individual optical sections
691 was used. Aniline blue fluorescence was excited at 405 nm using a diode laser and
692 detected at 425 to 525 nm. H_2DCFDA and EGFP fluorescence excitation was done at
693 488 nm using a multi-line argon laser and detected at 502 to 536 nm. For the direct
694 comparisons of fluorescence intensities, laser, pinhole and gain settings of the
695 confocal microscope were kept identical when capturing the images from the
696 seedlings of different treatments. Scan speeds were set at 400 Hz and line averages at
697 between 2 and 4. Measurements on digital micrographs were done using ImageJ
698 software [76]. Images were adjusted for color and contrast using Adobe Photoshop

699 CC software (Adobe, San Jose, USA).

700

701 ## Acknowledgments

702 We acknowledge Ramon Torres Ruiz and other members of the Schneitz lab for
703 helpful discussion and suggestions. We thank Herman Höfte for *the1* alleles. We also
704 thank Lynette Fulton, Silke Robatzek, Martin Stegmann and Sebastian Wolf for
705 critical reading of the manuscript. We further acknowledge the support of the Center
706 for Advanced Light Microscopy (CALM) at the TUM School of Life Sciences. This
707 work was funded by the German Research Council (DFG) through grants SFB924
708 (TP B12) to CD and SFB924 (TP A2) to KS.

709

710 ## AUTHOR CONTRIBUTIONS

711 A.C., C.D. and K.S. designed the research. A.C., X.C., J.G., B.L. and R.H. performed
712 research. A.C., X.C., J.G., B.L., C.D. and K.S. analyzed the data. K.S. wrote the
713 paper.

714

715 ## References

716 1. Lampugnani ER, Khan GA, Somssich M, Persson S (2018) Building a plant cell
717 wall at a glance. J Cell Sci 131:
718 2. Höfte H, Voxeur A (2017) Plant cell walls. Current Biology 27: R865-R870.
719 3. Cosgrove DJ (2016) Plant cell wall extensibility: connecting plant cell growth
720 with cell wall structure, mechanics, and the action of wall-modifying enzymes. J
721 Exp Bot 67: 463-476.
722 4. Boller T, Felix G (2009) A renaissance of elicitors: perception of microbe-
723 associated molecular patterns and danger signals by pattern-recognition
724 receptors. Annu Rev Plant Biol 60: 379-406.

5. Franck CM, Westermann J, Boisson-Dernier A (2018) Plant malectin-like receptor kinases: from cell wall integrity to immunity and beyond. Annu Rev Plant Biol 69: 301-328.
6. Voxeur A, Höfte H (2016) Cell wall integrity signaling in plants: "To grow or not to grow that's the question". Glycobiology 26: 950-960.
7. Wolf S (2017) Plant cell wall signalling and receptor-like kinases. Biochem J 474: 471-492.
8. Wolf S, van der Does D, Ladwig F, Sticht C, Kolbeck A, Schurholz AK et al. (2014) A receptor-like protein mediates the response to pectin modification by activating brassinosteroid signaling. Proc Natl Acad Sci U S A 111: 15261-15266.
9. Wolf S, Mravec J, Greiner S, Mouille G, Höfte H (2012) Plant cell wall homeostasis is mediated by brassinosteroid feedback signaling. Curr Biol 22: 1732-1737.
10. Escobar-Restrepo JM, Huck N, Kessler S, Gagliardini V, Gheyselinck J, Yang WC et al. (2007) The FERONIA receptor-like kinase mediates male-female interactions during pollen tube reception. Science 317: 656-660.
11. Feng W, Kita D, Peaucelle A, Cartwright HN, Doan V, Duan Q et al. (2018) The FERONIA receptor kinase maintains cell-wall integrity during salt stress through Ca2+ signaling. Curr Biol 28: 666-675.e5.
12. Boisson-Dernier A, Roy S, Kritas K, Grobei MA, Jaciubek M, Schroeder JI et al. (2009) Disruption of the pollen-expressed FERONIA homologs ANXUR1 and ANXUR2 triggers pollen tube discharge. Development 136: 3279-3288.
13. Franck C, Westermann J, Bürssner S, Lentz R, Lituiev DS, Boisson-Dernier A (2018) The protein phosphatases ATUNIS1 and ATUNIS2 regulate cell wall integrity in tip-growing cells. Plant Cell
14. Mecchia MA, Santos-Fernandez G, Duss NN, Somoza SC, Boisson-Dernier A, Gagliardini V et al. (2017) RALF4/19 peptides interact with LRX proteins to control pollen tube growth in Arabidopsis. Science
15. Miyazaki S, Murata T, Sakurai-Ozato N, Kubo M, Demura T, Fukuda H et al. (2009) ANXUR1 and 2, sister genes to FERONIA/SIRENE, are male factors for coordinated fertilization. Curr Biol 19: 1327-1331.

16. Somerville C, Bauer S, Brininstool G, Facette M, Hamann T, Milne J et al. (2004) Toward a systems approach to understanding plant cell walls. Science 306: 2206-2211.
17. Caño-Delgado A, Penfield S, Smith C, Catley M, Bevan M (2003) Reduced cellulose synthesis invokes lignification and defense responses in Arabidopsis thaliana. Plant J 34: 351-362.
18. Cano-Delgado AI, Metzlaff K, Bevan MW (2000) The eli1 mutation reveals a link between cell expansion and secondary cell wall formation in Arabidopsis thaliana. Development 127: 3395-3405.
19. Ellis C, Karafyllidis I, Wasternack C, Turner JG (2002) The Arabidopsis mutant cev1 links cell wall signaling to jasmonate and ethylene responses. Plant Cell 14: 1557-1566.
20. Ellis C, Turner JG (2001) The Arabidopsis mutant cev1 has constitutively active jasmonate and ethylene signal pathways and enhanced resistance to pathogens. Plant Cell 13: 1025-1033.
21. Fagard M, Desnos T, Desprez T, Goubet F, Refregier G, Mouille G et al. (2000) PROCUSTE1 encodes a cellulose synthase required for normal cell elongation specifically in roots and dark-grown hypocotyls of Arabidopsis. Plant Cell 12: 2409-2424.
22. Heim DR, Skomp JR, Tschabold EE, Larrinua IM (1990) Isoxaben Inhibits the Synthesis of Acid Insoluble Cell Wall Materials In Arabidopsis thaliana. Plant Physiol 93: 695-700.
23. Lefebvre A, Maizonnier D, Gaudry JC, Clair D, Scalla R (1987) Some effects of the herbicide EL-107 on cellular growth and metabolism. Weed Research 27: 125-134.
24. Desprez T, Vernhettes S, Fagard M, Refrégier G, Desnos T, Aletti E et al. (2002) Resistance against herbicide isoxaben and cellulose deficiency caused by distinct mutations in same cellulose synthase isoform CESA6. Plant Physiol 128: 482-490.
25. Scheible WR, Eshed R, Richmond T, Delmer D, Somerville C (2001) Modifications of cellulose synthase confer resistance to isoxaben and thiazolidinone herbicides in Arabidopsis Ixr1 mutants. Proc Natl Acad Sci U S A 98: 10079-10084.

790 26. Paredez AR, Somerville CR, Ehrhardt DW (2006) Visualization of cellulose
791 synthase demonstrates functional association with microtubules. Science 312:
792 1491-1495.
793 27. Heim DR, Skomp JR, Waldron C, Larrinua IM (1991) Differential response to
794 isoxaben of cellulose biosynthesis by wild-type and resistant strains of
795 Arabidopsis thaliana. Pesticide Biochemistry and Physiology 39: 93-99.
796 28. Engelsdorf T, Gigli-Bisceglia N, Veerabagu M, McKenna JF, Vaahtera L,
797 Augstein F et al. (2018) The plant cell wall integrity maintenance and immune
798 signaling systems cooperate to control stress responses in Arabidopsis thaliana.
799 Sci Signal 11:
800 29. Hamann T (2015) The plant cell wall integrity maintenance mechanism--a case
801 study of a cell wall plasma membrane signaling network. Phytochemistry 112:
802 100-109.
803 30. Wormit A, Butt SM, Chairam I, McKenna JF, Nunes-Nesi A, Kjaer L et al.
804 (2012) Osmosensitive changes of carbohydrate metabolism in response to
805 cellulose biosynthesis inhibition. Plant Physiol 159: 105-117.
806 31. Hamann T, Bennett M, Mansfield J, Somerville C (2009) Identification of cell-
807 wall stress as a hexose-dependent and osmosensitive regulator of plant
808 responses. Plant J 57: 1015-1026.
809 32. Hématy K, Sado PE, Van Tuinen A, Rochange S, Desnos T, Balzergue S et al.
810 (2007) A receptor-like kinase mediates the response of Arabidopsis cells to the
811 inhibition of cellulose synthesis. Curr Biol 17: 922-931.
812 33. Van der Does D, Boutrot F, Engelsdorf T, Rhodes J, McKenna JF, Vernhettes S
813 et al. (2017) The Arabidopsis leucine-rich repeat receptor kinase MIK2/LRR-
814 KISS connects cell wall integrity sensing, root growth and response to abiotic
815 and biotic stresses. PLoS Genet 13: e1006832.
816 34. Julkowska M, Koevoets IT, Mol S, Hoefsloot HC, Feron R, Tester M et al.
817 (2017) Genetic components of root architecture remodeling in response to salt
818 stress. Plant Cell
819 35. Wang T, Liang L, Xue Y, Jia PF, Chen W, Zhang MX et al. (2016) A receptor
820 heteromer mediates the male perception of female attractants in plants. Nature
821 531: 241-244.

822 36. Xu SL, Rahman A, Baskin TI, Kieber JJ (2008) Two leucine-rich repeat
823 receptor kinases mediate signaling, linking cell wall biosynthesis and ACC
824 synthase in Arabidopsis. Plant Cell 20: 3065-3079.
825 37. Gonneau M, Desprez T, Martin M, Doblas VG, Bacete L, Miart F et al. (2018)
826 Receptor kinase THESEUS1 Is a Rapid Alkalinization Factor 34 Receptor in
827 *Arabidopsis*. Curr Biol 28: 2452-2458.e4.
828 38. Chevalier D, Batoux M, Fulton L, Pfister K, Yadav RK, Schellenberg M et al.
829 (2005) *STRUBBELIG* defines a receptor kinase-mediated signaling pathway
830 regulating organ development in *Arabidopsis*. Proc Natl Acad Sci U S A 102:
831 9074-9079.
832 39. Kwak SH, Shen R, Schiefelbein J (2005) Positional signaling mediated by a
833 receptor-like kinase in *Arabidopsis*. Science 307: 1111-1113.
834 40. Lin L, Zhong SH, Cui XF, Li J, He ZH (2012) Characterization of temperature-
835 sensitive mutants reveals a role for receptor-like kinase
836 SCRAMBLED/STRUBBELIG in coordinating cell proliferation and
837 differentiation during Arabidopsis leaf development. Plant J 72: 707-720.
838 41. Vaddepalli P, Fulton L, Batoux M, Yadav RK, Schneitz K (2011) Structure-
839 function analysis of STRUBBELIG, an Arabidopsis atypical receptor-like
840 kinase involved in tissue morphogenesis. PLoS One 6: e19730.
841 42. Sager RE, Lee JY (2018) Plasmodesmata at a glance. J Cell Sci 131: jcs209346.
842 43. Otero S, Helariutta Y, Benitez-Alfonso Y (2016) Symplastic communication in
843 organ formation and tissue patterning. Curr Opin Plant Biol 29: 21-28.
844 44. Vaddepalli P, Herrmann A, Fulton L, Oelschner M, Hillmer S, Stratil TF et al.
845 (2014) The C2-domain protein QUIRKY and the receptor-like kinase
846 STRUBBELIG localize to plasmodesmata and mediate tissue morphogenesis in
847 *Arabidopsis thaliana*. Development 141: 4139-4148.
848 45. Fulton L, Batoux M, Vaddepalli P, Yadav RK, Busch W, Andersen SU et al.
849 (2009) DETORQUEO, QUIRKY, and ZERZAUST represent novel components
850 involved in organ development mediated by the receptor-like kinase
851 STRUBBELIG in Arabidopsis thaliana. PLoS Genet 5: e1000355.
852 46. Vaddepalli P, Fulton L, Wieland J, Wassmer K, Schaeffer M, Ranf S et al.
853 (2017) The cell wall-localized atypical β-1,3 glucanase ZERZAUST controls
854 tissue morphogenesis in *Arabidopsis thaliana*. Development 144: 2259-2269.

855 47. Desprez T, Juraniec M, Crowell EF, Jouy H, Pochylova Z, Parcy F et al. (2007)
856 Organization of cellulose synthase complexes involved in primary cell wall
857 synthesis in Arabidopsis thaliana. Proc Natl Acad Sci U S A
858 48. Persson S, Paredez A, Carroll A, Palsdottir H, Doblin M, Poindexter P et al.
859 (2007) Genetic evidence for three unique components in primary cell-wall
860 cellulose synthase complexes in Arabidopsis. Proc Natl Acad Sci U S A
861 49. Henry E, Fung N, Liu J, Drakakaki G, Coaker G (2015) Beyond glycolysis:
862 GAPDHs are multi-functional enzymes involved in regulation of ros, autophagy,
863 and plant immune responses. PLoS Genet 11: e1005199.
864 50. Juárez SP, Mangano S, Estevez JM (2015) Improved ROS measurement in root
865 hair cells. Methods Mol Biol 1242: 67-71.
866 51. Schenk ST, Schikora A (2015) Staining of callose depositions in root and leaf
867 tissues. Bio-protocol 5: e1429.
868 52. Heim DR, Roberts JL, Pike PD, Larrinua IM (1990) A second locus, Ixr B1 in
869 Arabidopsis thaliana, that confers resistance to the herbicide isoxaben. Plant
870 Physiol 92: 858-861.
871 53. Trehin C, Schrempp S, Chauvet A, Berne-Dedieu A, Thierry AM, Faure JE et
872 al. (2013) QUIRKY interacts with STRUBBELIG and PAL OF QUIRKY to
873 regulate cell growth anisotropy during Arabidopsis gynoecium development.
874 Development 140: 4807-4817.
875 54. Song JH, Kwak SH, Nam KH, Schiefelbein J, Lee MM (2019) QUIRKY
876 regulates root epidermal cell patterning through stabilizing SCRAMBLED to
877 control CAPRICE movement in Arabidopsis. Nat Commun 10: 1744.
878 55. Sampathkumar A, Yan A, Krupinski P, Meyerowitz EM (2014) Physical forces
879 regulate plant development and morphogenesis. Curr Biol 24: R475-83.
880 56. Kwak SH, Woo S, Lee MM, Schiefelbein J (2014) Distinct signaling
881 mechanisms in multiple developmental pathways by the SCRAMBLED receptor
882 of Arabidopsis. Plant Physiol 166: 976-987.
883 57. Denness L, McKenna JF, Segonzac C, Wormit A, Madhou P, Bennett M et al.
884 (2011) Cell wall damage-induced lignin biosynthesis is regulated by a reactive
885 oxygen species- and jasmonic acid-dependent process in Arabidopsis. Plant
886 Physiol 156: 1364-1374.

887 58. Kohorn BD, Kobayashi M, Johansen S, Riese J, Huang LF, Koch K et al. (2006)
888 An Arabidopsis cell wall-associated kinase required for invertase activity and
889 cell growth. Plant J 46: 307-316.
890 59. Engelsdorf T, Hamann T (2014) An update on receptor-like kinase involvement
891 in the maintenance of plant cell wall integrity. Ann Bot 114: 1339-1347.
892 60. Haswell ES, Verslues PE (2015) The ongoing search for the molecular basis of
893 plant osmosensing. J Gen Physiol 145: 389-394.
894 61. Nissen KS, Willats WGT, Malinovsky FG (2016) Understanding CrRLK1L
895 Function: Cell Walls and Growth Control. Trends Plant Sci 21: 516-527.
896 62. He Y, Zhou J, Shan L, Meng X (2018) Plant cell surface receptor-mediated
897 signaling - a common theme amid diversity. J Cell Sci 131: 1-11.
898 63. Ma X, Xu G, He P, Shan L (2016) SERKing Coreceptors for Receptors. Trends
899 Plant Sci 21: 1017-1033.
900 64. Schwessinger B, Roux M, Kadota Y, Ntoukakis V, Sklenar J, Jones A et al.
901 (2011) Phosphorylation-dependent differential regulation of plant growth, cell
902 death, and innate immunity by the regulatory receptor-like kinase BAK1. PLoS
903 Genet 7: e1002046.
904 65. Perraki A, DeFalco TA, Derbyshire P, Avila J, Séré D, Sklenar J et al. (2018)
905 Phosphocode-dependent functional dichotomy of a common co-receptor in plant
906 signalling. Nature
907 66. Cao Y, Liang Y, Tanaka K, Nguyen CT, Jedrzejczak RP, Joachimiak A et al.
908 (2014) The kinase LYK5 is a major chitin receptor in *Arabidopsis* and forms a
909 chitin-induced complex with related kinase CERK1. Elife 3:
910 67. Stegmann M, Monaghan J, Smakowska-Luzan E, Rovenich H, Lehner A,
911 Holton N et al. (2017) The receptor kinase FER is a RALF-regulated scaffold
912 controlling plant immune signaling. Science 355: 287-289.
913 68. Wang ZP, Xing HL, Dong L, Zhang HY, Han CY, Wang XC et al. (2015) Egg
914 cell-specific promoter-controlled CRISPR/Cas9 efficiently generates
915 homozygous mutants for multiple target genes in Arabidopsis in a single
916 generation. Genome Biol 16: 144.
917 69. Xie K, Zhang J, Yang Y (2014) Genome-wide prediction of highly specific
918 guide RNA spacers for CRISPR-Cas9-mediated genome editing in model plants
919 and major crops. Mol Plant 7: 923-926.

70. Koncz C, Schell J (1986) The promoter of TL-DNA gene 5 controls the tissue-specific expression of chimaeric genes carried by a novel type of *Agrobacterium* binary vector. Mol Gen Genet 204: 383-396.
71. Clough SJ, Bent AF (1998) Floral dip: a simplified method for Agrobacterium-mediated transformation of Arabidopsis thaliana. Plant J 16: 735-743.
72. Kumar M, Turner S (2015) Protocol: a medium-throughput method for determination of cellulose content from single stem pieces of Arabidopsis thaliana. Plant Methods 11: 46.
73. Updegraff DM (1969) Semimicro determination of cellulose inbiological materials. Anal Biochem 32: 420-424.
74. Box MS, Coustham V, Dean C, Mylne JS (2011) Protocol: A simple phenol-based method for 96-well extraction of high quality RNA from Arabidopsis. Plant Methods 7: 7.
75. Enugutti B, Kirchhelle C, Oelschner M, Torres Ruiz RA, Schliebner I, Leister D et al. (2012) Regulation of planar growth by the Arabidopsis AGC protein kinase UNICORN. Proc Natl Acad Sci U S A 109: 15060-15065.
76. Rueden CT, Schindelin J, Hiner MC, DeZonia BE, Walter AE, Arena ET et al. (2017) ImageJ2: ImageJ for the next generation of scientific image data. BMC Bioinformatics 18: 529.

Figures

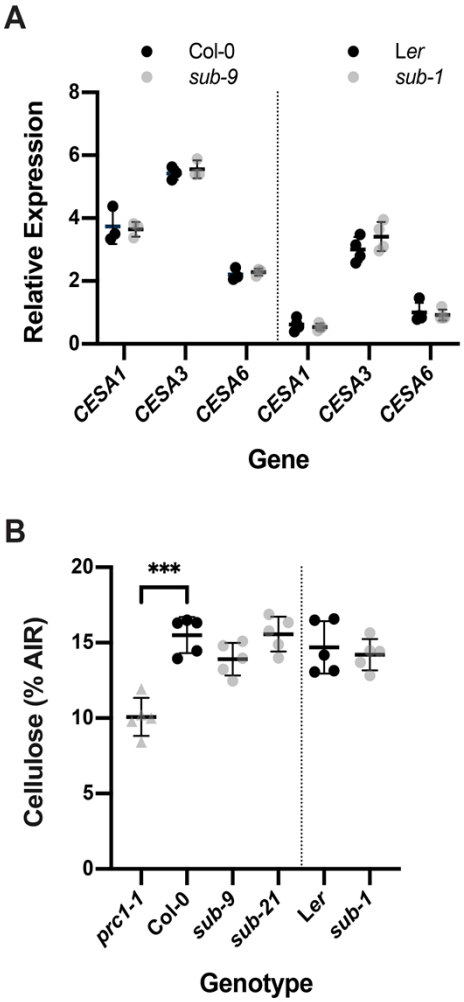

Fig 1. Effects of *SUB* on cellulose content in seven-day-old seedlings. (A) Gene expression levels for primary cell wall *CESA* genes in wild type and *sub* as assessed by qPCR. Individual *CESA* genes and genotypes are indicated. Mean ± SD is shown. Data points designate results of individual biological replicates. The experiment was performed two times with similar results. (B) Estimation of cellulose content. Genotypes are indicated. Data points indicate results of individual biological replicates. Mean ± SD is shown. Asterisks represent statistical significance ($P < 0.0001$, unpaired t test, two-tailed P values). No significant difference was observed between wild type and different *sub* mutants. Plants with a defect in *CESA6* (*prc1-1*)

962 show a reduction in cellulose content as previously reported [21]. The experiment was

963 repeated three times with similar results.

964

965

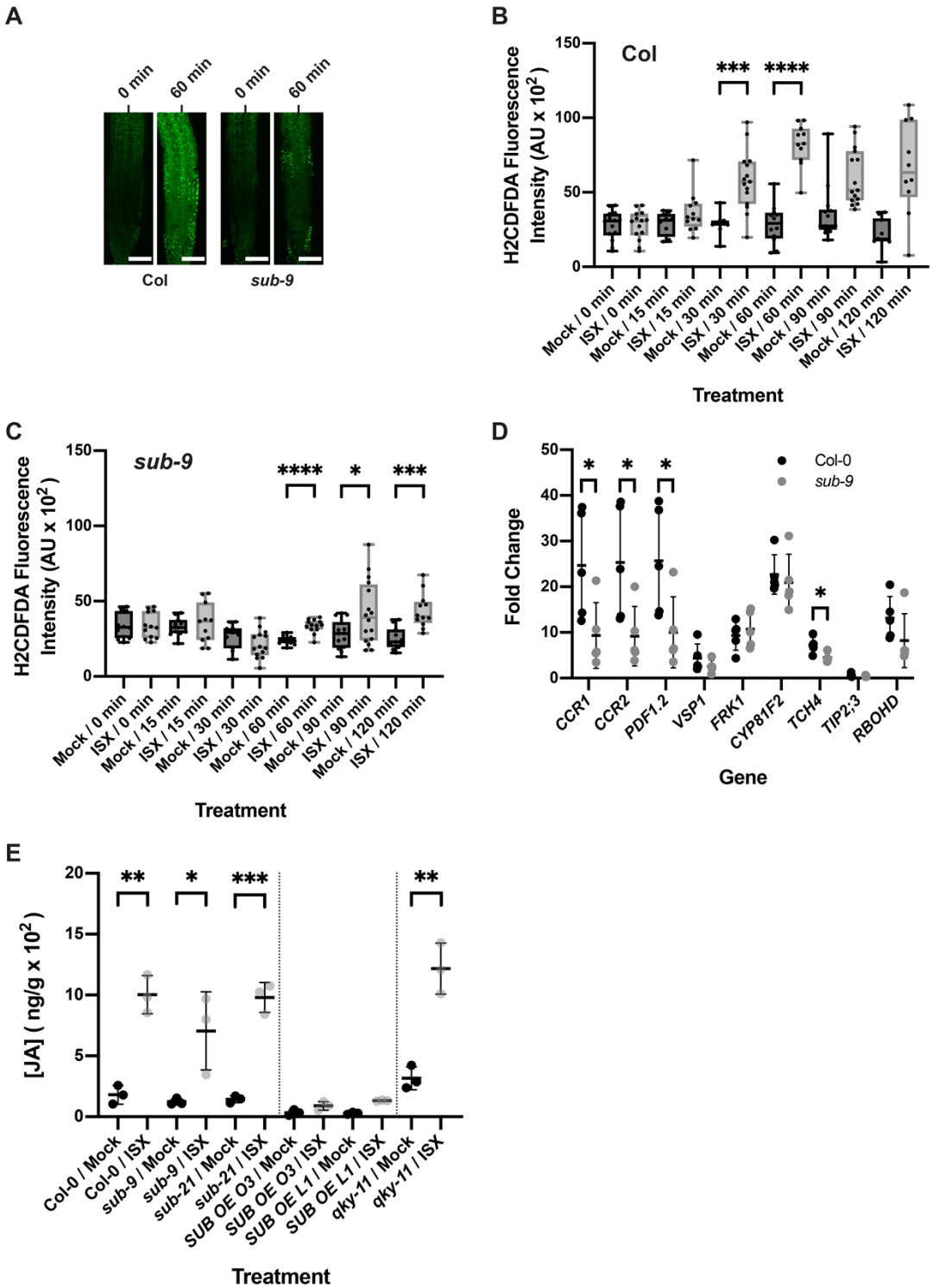

966

967 **Fig. 2. *SUB* effects on isoxaben-induced ROS production, marker gene**
968 **expression and JA accumulation.** (A) Confocal micrographs showing H_2CFDA
969 signal in root tips of six-day-old seedlings exposed to 600 nM isoxaben for the
970 specified time. Genotypes are indicated. Note reduced signal in *sub-9*. (B, C)
971 Quantification of results depicted in (A). Genotypes are indicated. Box and whisker
972 plots are shown. $10 \leq n \leq 14$. Asterisks represent statistical significance ($_{****}$, $P <$
973 0.0001; $_{***}$ $P < 0.002$, $_{*}$ $P < 0.05$, unpaired t test, two-tailed P values). Experiments
974 were performed three times with similar results. (D) Gene expression levels of several
975 CBI marker genes by qPCR upon exposure of seven-day-old seedlings to 600 nM
976 isoxaben for eight hours. The results from five biological replicates are shown.
977 Marker genes and genotypes are indicated. Mean ± SD is presented. Asterisks
978 represent statistical significance ($_{*}$, $P < 0.05$, unpaired t test, two-tailed P values). The
979 experiment was repeated twice with similar results. (E) JA accumulation. Genotypes
980 and treatments are indicated. Asterisks represent statistical significance ($_{***}$, $P <$
981 0.002; $_{**}$, $P < 0.003$; $_{*}$ $P < 0.05$, unpaired t test, two-tailed P values). $n = 3$.
982 Experiments were repeated three times with similar results. Scale bars: (A) 100 µm.
983
984

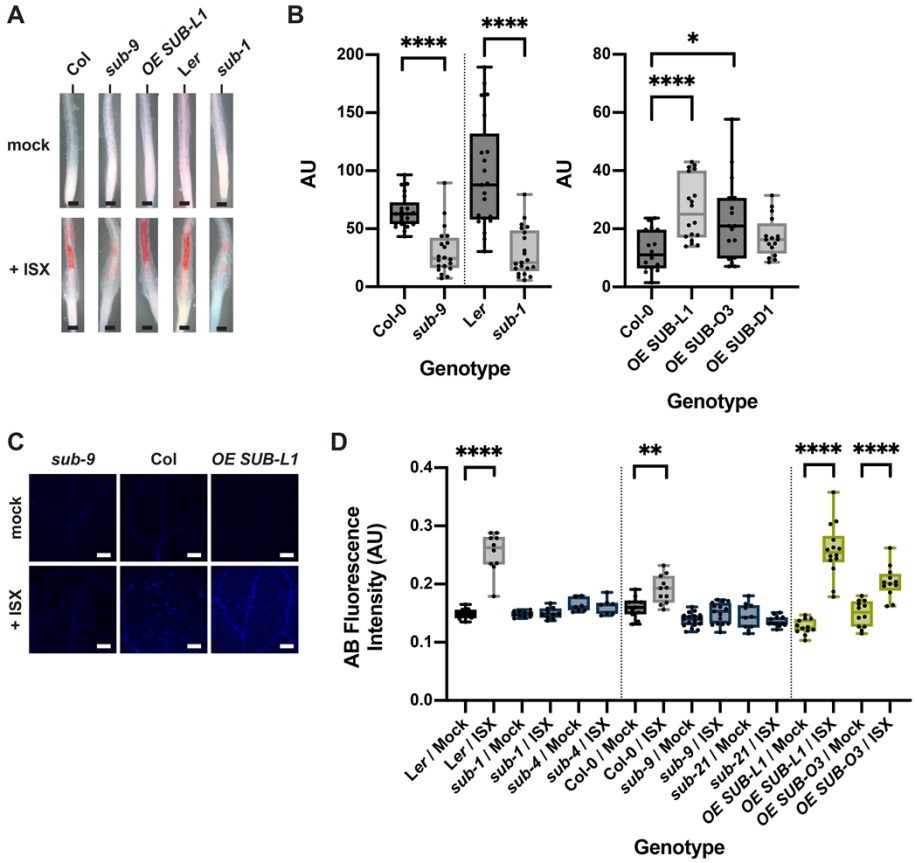

985

986 **Fig. 3. *SUB* affects isoxaben-induced lignin and callose accumulation.** (A)

987 Phloroglucinol signal strength indicating lignin accumulation in roots of six-day-old

988 seedlings exposed to 600 nM isoxaben for 12 hours. Genotypes: Col, *sub-9* (Col),

989 *pUBQ::gSUB:mCherry* (line L1), L*er*, and *sub-1* (L*er*). (B) Quantification of the

990 results depicted in (A). Left panel shows results obtained from different *sub* mutants

991 in the Col or L*er* background. Right panel depicts results from three independent

992 *pUBQ::gSUB:mCherry* transgenic lines overexpressing *SUB* (Col, lines L1, O3, D1).

993 Box and whisker plots are shown. $16 \leq n \leq 21$. Asterisks represent statistical

994 significance ($*$ $P < 0.02$, $****$, $P < 0.0001$; unpaired t test, two-tailed P values). The

995 experiment was performed three times with similar results. (C) Confocal micrographs

996 show cotyledons of seven-day-old *sub-9*, Col, and *pUBQ::gSUB:mCherry* (line L1)

997 seedlings treated with mock or 600 nM isoxaben for 24 hours. Aniline blue

998 fluorescence signal strength indicates callose accumulation. (D) Quantification of the

999 results depicted in (C). Left panel shows results obtained from *sub* mutants in L*er*
1000 background. Center panels indicates results obtained from *sub* mutants in Col
1001 background. Right panel depicts results from two independent *pUBQ::gSUB:mCherry*
1002 transgenic lines overexpressing *SUB* (Col, lines L1, O3). Box and whisker plots are
1003 shown. $7 \leq n \leq 18$. Asterisks represent statistical significance (****, $P < 0.0001$; ** $P <$
1004 0.004, unpaired t test, two-tailed P values). The experiment was performed three times
1005 with similar results. Scale bars: (A) 0.1 mm; (C) 0.2 mm.
1006
1007

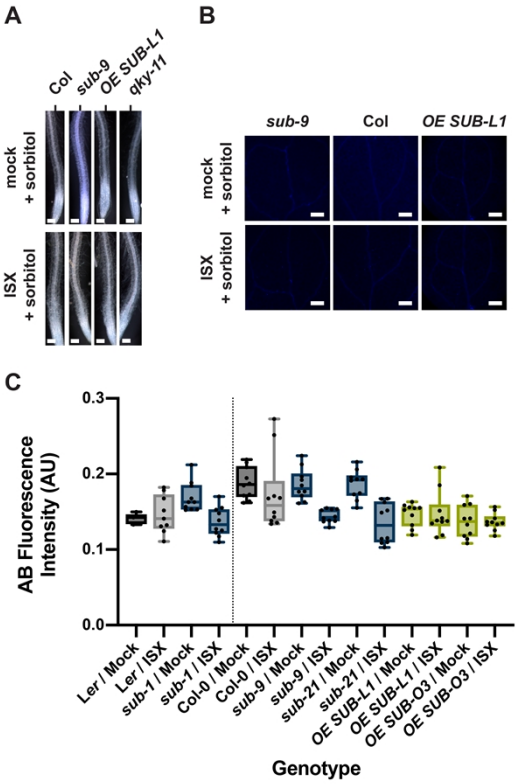

1008

1009 **Fig. 4. The effects of sorbitol on lignin and callose accumulation upon isoxaben**
1010 **exposure.** (A) Phloroglucinol signal strength indicating lignin accumulation in roots
1011 of six-day-old seedlings exposed to mock/300 mM sorbitol or to 600 nM
1012 isoxaben/300 mM sorbitol for 12 hours. Genotypes: Col, *sub-9* (Col),
1013 *pUBQ::gSUB:mCherry* (line L1), *qky-11* (Col). Note absence of detectable signal.

The experiment was performed three times with similar results ($n \geq 10$). (B) Confocal micrographs show cotyledons of seven-day-old *sub-9*, Col, and *pUBQ::gSUB:mCherry* (Col, line L1) seedlings treated with mock/300 mM sorbitol or 600 nM isoxaben/300 mM sorbitol for 24 hours. Aniline blue fluorescence signal strength indicates callose accumulation. No increase in signal intensity can be observed in isoxaben-treated seedlings. (C) Quantification of the results depicted in (B). Left panel depicts results obtained from *sub-1* mutants in L*er* background. Right panel shows results obtained from *sub* mutants in Col background and also depicts results from two independent *pUBQ::gSUB:mCherry* transgenic lines overexpressing *SUB* (Col, lines L1, O3). Box and whisker plots are shown. $5 \leq n \leq 10$. No statistically significant differences were observed (unpaired t tests, two-tailed P values). The experiment was performed three times with similar results. Scale bars: (A) 0.1 mm; (C) 0.2 mm.

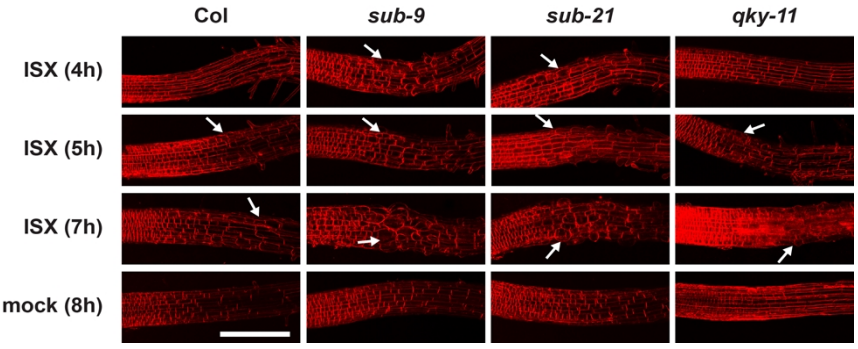

Fig. 5. Root epidermal cell shape changes upon isoxaben treatment. Six-day-old seedlings counter-stained with the membrane stain FM4-64 are shown. Confocal micrographs depict the region where the elongation zone flanks the root meristem. Time of exposure in hours to 600 nM isoxaben (ISX) or mock is indicated as are the genotypes. Arrows denote aberrant cell shapes. Scale bar: 0.1 mm.

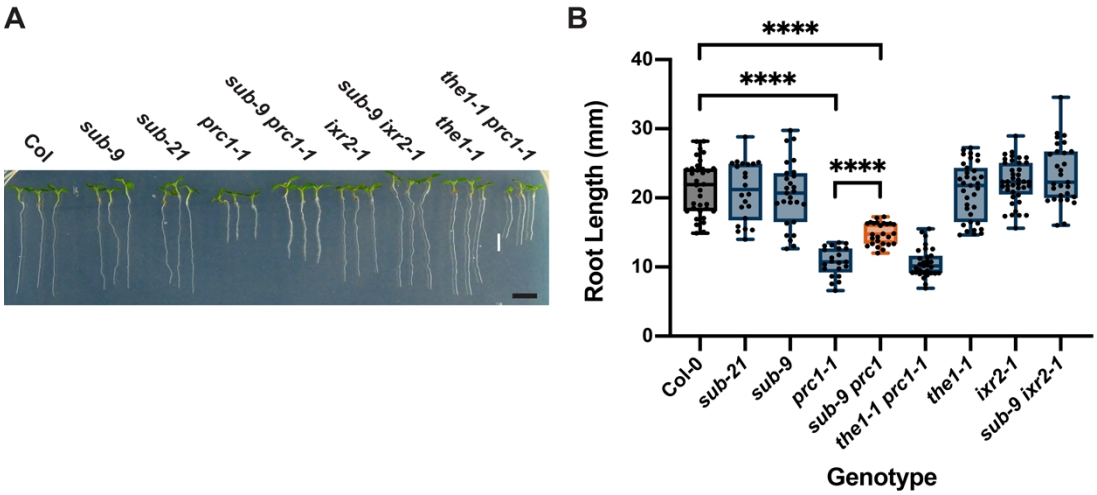

Fig. 6. *SUB* effect on root growth inhibition in *prc1-1*. (A) Root length in seven-day-old seedlings grown on plates under long-day conditions (16 hours light). Genotypes are indicated. Note the partial rescue of root length in *sub-9 prc1-1* but not in *the1-1 prc1-1*. (B) Quantification of the data shown in (A). Box and whisker plots are shown. $21 \leq n \leq 40$. Asterisks represent statistical significance (****, $P < 0.0001$; unpaired t test, two-tailed P values). The experiment was performed three times with similar results. Scale bars: 0.5 mm.

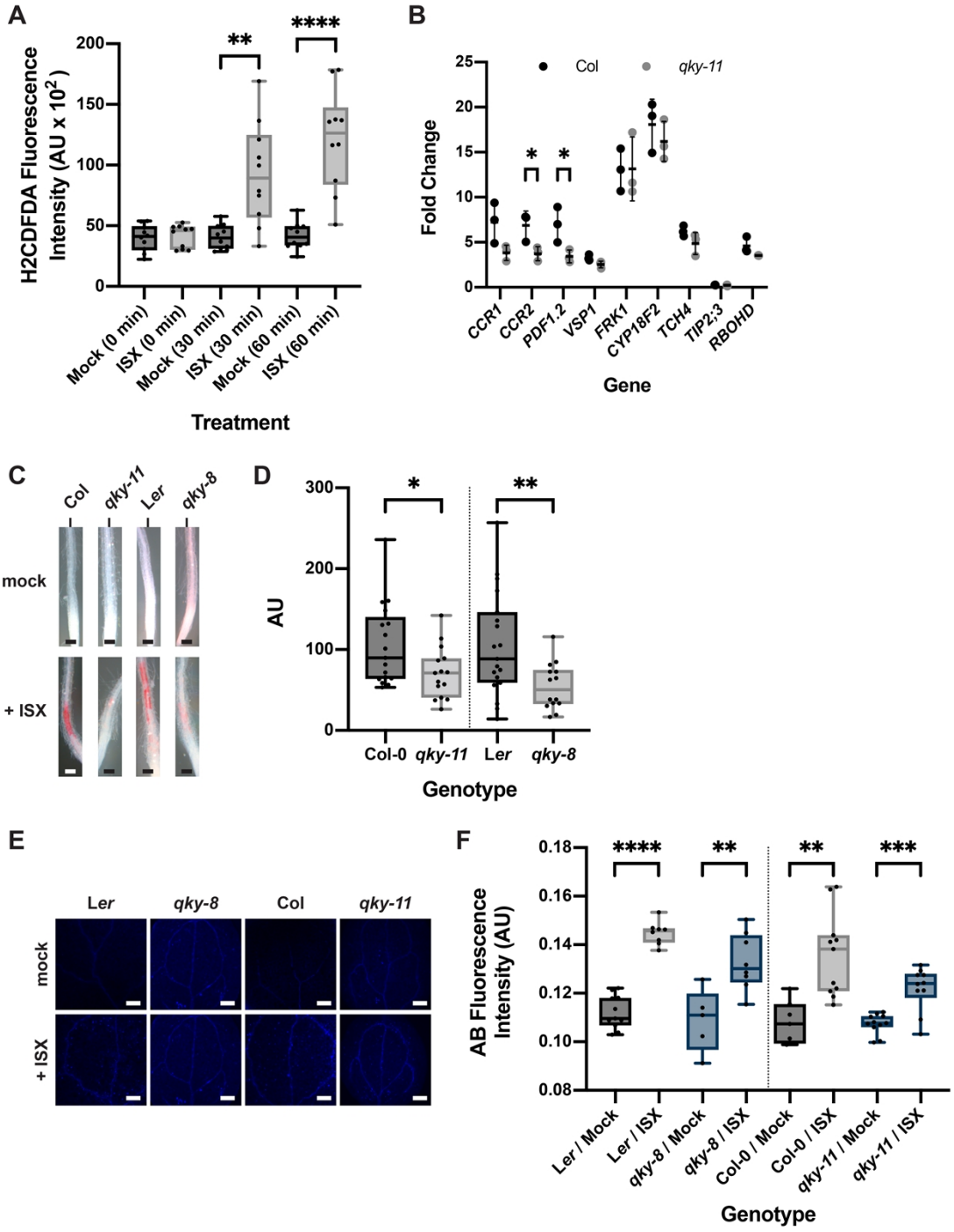

1047

1048 **Fig. 7. Role of *QKY* in isoxaben-induced CBI responses.** (A) Quantification of

1049 H_2CDFDA signal indicating ROS accumulation in root tips of six-day-old *qky-11*

1050 seedlings exposed to mock or 600 nM isoxaben for the indicated time. Note the

1051 unaltered signal. Box and whisker plots are shown. n = 10. Asterisks represent

1052 statistical significance (**, P = 0.0013; ****, P < 0.0001, unpaired t test, two-tailed P

1053 values). Experiments were performed three times with similar results. (B) Gene

expression levels of several CBI marker genes by qPCR upon exposure of seven-day-old seedlings to 600 nM isoxaben for eight hours. The results from three biological replicates are shown. Marker genes and genotypes are indicated. Mean ± SD is presented. Asterisks represent statistical significance ($*$, $P < 0.05$, unpaired t test, two-tailed P values). The experiment was repeated three times with similar results. (C) Phloroglucinol signal strength indicating lignin accumulation in roots of six-day-old seedlings exposed to 600 nM isoxaben for 12 hours. Genotypes: Col, *qky-11* (Col), L*er*, and *sub-1* (L*er*). (D) Quantification of the results depicted in (C). Genotypes are indicated. Box and whisker plots are shown. $15 \leq n \leq 19$. Asterisks represent statistical significance ($*$ $P < 0.04$, $**$, $P < 0.01$; unpaired t test, two-tailed P values). The experiment was performed three times with similar results. (E) Confocal micrographs show cotyledons of seven-day-old L*er*, *qky-8* (L*er*), Col, and *qky-11* (Col) seedlings treated with mock or 600 nM isoxaben for 24 hours. Aniline blue fluorescence signal strength indicates callose accumulation. (F) Quantification of the results depicted in (E). Left panel shows results obtained from *qky-8* mutants in L*er* background. Right panel indicates results obtained from *qky-11* mutants in Col background. Box and whisker plots are shown. $5 \leq n \leq 11$. Asterisks represent statistical significance ($**$ $P < 0.006$, ***, $P = 0.0001$; $****$, $P < 0.0001$; unpaired t test, two-tailed P values). The experiment was performed three times with similar results. Scale bars: (C) 0.1 mm; (E) 0.2 mm.

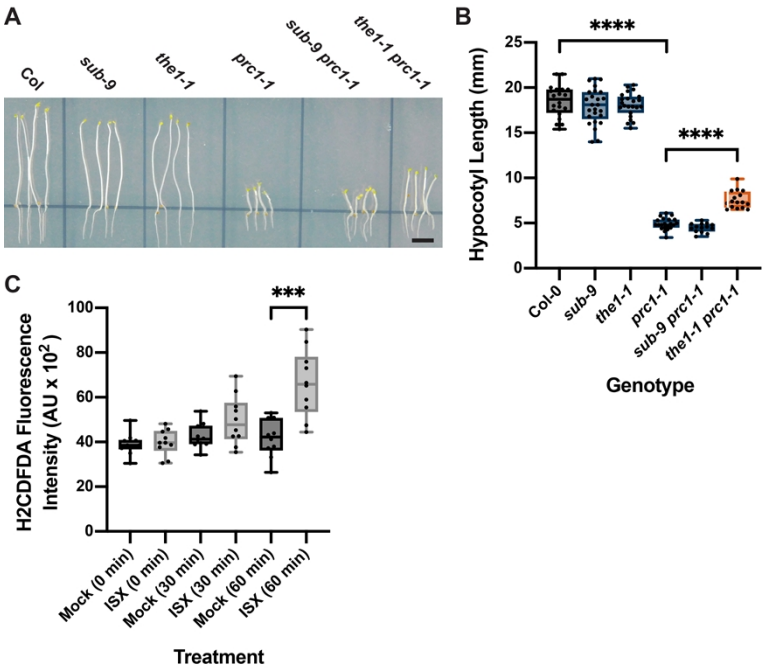

Fig. 8. Influence of *THE1* on etiolated hypocotyl length of *prc1-1* and isoxaben-induced ROS accumulation in root tips. (A) Hypocotyl elongation in six-day-old seedlings grown on plates in the dark. Genotypes are indicated. Note the partial rescue of hypocotyl elongation in *the1-1 prc1-1* but not in *sub-9 prc1-1*. (B) Quantification of the data shown in (A). Box and whisker plots are shown. $14 \leq n \leq 25$. Asterisks represent statistical significance (****, $P < 0.0001$; unpaired t test, two-tailed P values). The experiment was performed three times with similar results. (C) Quantification of H_2CDFDA signal indicating ROS accumulation in root tips of six-day-old *the1-1* seedlings exposed to mock or 600 nM isoxaben for the indicated time. Note the unaltered signal at 30 minutes exposure. Box and whisker plots are shown. $n = 10$. Asterisks represent statistical significance (***, $P = 0.0003$, unpaired t test, two-tailed P values). Experiments were performed three times with similar results. Scale bars: 0.5 mm.

Tables

Table 1. Root growth recovery after isoxaben treatment.

Genotype	N total[a]	24 h[b]	48 h[b]	72 h[b]
L*er*	110	45.5	69.1	85.5
sub-1	82	24.4**	50.0*	64.6**
sub-4	76	17.1**	39.5****	52.6****
qky-8	87	37.9ns	64.4ns	88.5ns
Col-0	142	38.7	65.5	90.1
sub-9	88	23.9*	45.5**	70.5**
sub-21	72	26.4ns	51.4ns	68.1**
qky-11	81	37.0ns	64.2ns	92.6ns
ixr2-1	83	97.6****	97.6****	97.6ns
sub-9 ixr2-1	77	100.0****	100.0****	100.0**
the1-1	78	41.0ns	69.2ns	88.5ns

Percentages of root growth recovery of plate-grown, seven-day-old seedlings after transient exposure to 600 nM isoxaben for 24 hours. The top four sample rows list genotypes that are in Ler background. The bottom seven sample rows list genotypes that are in Col background.

[a]Total number of samples. Cases per class and timepoint were pooled from three independent experiments. For each biological replicate $22 \leq n \leq 32$ seedlings were analyzed per genotype and time point.

[b]Statistical significance (mutant vs respective wild type): na, not applicable; ns, not significant; * $P < 0.05$; ** $P < 0.005$; **** $P < 0.0001$; (Fisher's exact test; two-sided).

Supporting information

1106 **S1 Fig. *SUB* affects isoxaben-dependent induction of *CCR1* and *PDF1.2*.**

1107 **Table S1. Primers used in this study.**

1108